ICIC Express Letters
Volume **10**, Number **3**, March **2016**

 ISSN 1881-803X
pp. **663–668**

NEAR-FIELD MULTIPLE SIGNAL CLASSIFICATION ALGORITHM FOR ACOUSTIC EMISSION SOURCE LOCALIZATION IN ROLLING ELEMENT RUB-IMPACT FAULT DIAGNOSTICS

Jing Li[1], Aidong Deng[2], Dongying Liu[2], Rui Zhang[2] and Li Zhao[1]

[1]School of Information Engineering
[2]National Engineering Research Center of Turbo-Generator Vibration
Southeast University
No. 2, Sipailou, Nanjing 210096, P. R. China
{ 230149053; dnh }@seu.edu.cn

Received September 2015; accepted December 2015

Abstract. *Rub-impact source localization is an important indicator to evaluate incipient faults in rotating machine. The accurate evaluation of damage location can assist in early warning of failure. This paper proposes a Near-Field Multiple Signal Classification method (NFM) to estimate the location of acoustic emission (AE) source in rub-impact, using an array of sensors closed placed in a local region. This method combines the Wavelet Packet Transform (WPT) for the zero order extensional (S_0) and flexural waves (A_0) extraction, Modal Plate Wave Theory (MPWT) analysis for the revised propagation velocity and NFM algorithm to find the AE source position. The localization accuracy of rubbing source based on NFM, time of arrival (TOA), Delta-T and delay time beamforming (DTB) methods are compared by rubbing test carried on a test rig of rotation machinery. The results indicate that the improved method can localize rub fault more reliable and efficient than the others and is a helpful analysis tool for rub-impact fault diagnosis.*

Keywords: Rub-impact, Acoustic emission, Near field, Multiple signal classification

1. **Introduction.** Condition monitoring systems for rotating machinery used in industries are vital to keep the plant at healthy condition for maximum production, detect incipient faults and avoid serious damages and accidents. The rotating machine rubbing emits acoustic energy and one of the advantages of acoustic emission (AE) testing is in-service inspection technique which can reduce downtime for inspection and extend run time between inspection and overhauls [1]. Due to its potential advantages, AE technique, as a kind of non-destructive testing tools, has expanded towards rub-impact fault diagnosis and sources localization of rotating machines.

AE source localization is an important reference to rub-impact monitoring between rotor and stator. AE source localization has been seen considerable academic interest in recent years. The conventional time of arrival (TOA) method in two-dimensional space, using the concept of triangulation to determine the origin of a source was explained in detail by Miller et al. [2,3]. The major defect, the location error is sensitive to some parameters such as preset AE signal threshold, Effective Velocity, noise, dispersion and energy attenuation during propagation process of waves [4]. Especially, the threshold effect caused by the first hit arrival and first threshold crossing may also hazard the location accuracy [5].

Baxter developed Delta-T mapping technique to minimize the velocity and geometry errors and improve the accuracy effectively. Nevertheless, it is noted that a map of constant Delta-T contours for sensors pairs must be calculated before the practical location and the sensor arrays must be unchanged [6].

Mohd et al. [7] presented wavelet transform analysis and modal localization (WTML) method using the time delay of the zero order extensional (S_0) and flexural (A_0) modal waves extracted from each AE event to minimize the threshold effect and achieve some better localization results than TOA method. Furthermore, it was considered as a more reliable and easier source localization methodology than Delta-T as no necessary test grid and H-N source for training data. However, the triangulation to locate AE source in WTML may also figure out erroneous results and confuse localization accuracy.

McLaskey et al. [8] investigated the damage of large structures in civil engineering by using AE delay time beamforming (DTB) method, which was the first application in AE source localization. It was also verified that beamforming method in AE source localization was a probable way to localize rub fault [9]. However, the localization accuracy is still threatened by the noise rooting in AE records.

This paper proposes a Near-Field Multiple Signal Classification (NFM) algorithm to alleviate the noise effect, combining Wavelet Packet Transform (WPT) analysis with Modal Plate Wave Theory (MPWT) to revise velocity and improve the localization accuracy of rub-impact source in rolling element. The rest of this paper is organized as the following. First, we briefly analyze MPWT for the pre-processing of AE signals dispersion in steel plate in Section 2. Then the proposed model for AE source localization is presented in Section 3. Section 4 shows the experimental results in detail. Finally, we conclude this paper in Section 5.

2. **Dispersion Relation of MPWT.** The steel plate thickness, 10mm, is much shorter than the acoustic wavelength. The equations from plate theory can be used to explain the propagation characteristics of AE signal [10].

Equation (1) and Equation (2) indicate the dispersion equations of extensional wave (S) and flexural wave (A) respectively. Here p and q are two temporary variables, c_p is the propagation velocity of longitudinal wave, c_s is the propagation velocity of shear wave, k is the wave number, c is the phase velocity, c_g is the group velocity, h is the half thickness of plate and ω is the circular frequency.

$$\frac{\tan(qh)}{\tan(ph)} = -\frac{4k^2pq}{(q^2-k^2)^2} \tag{1}$$

$$\frac{\tan(qh)}{\tan(ph)} = -\frac{(q^2-k^2)^2}{4k^2pq} \tag{2}$$

$$p^2 = \frac{\omega^2}{c_p^2} - k^2, \quad q^2 = \frac{\omega^2}{c_s^2} - k^2, \quad k = \frac{\omega}{c}, \quad c_g = \frac{\partial\omega}{\partial k}$$

The dispersion curves can be obtained by the numerical solutions of Equation (1) and Equation (2) using dichotomy [11]. Figure 1 describes four modes dispersion curves where c_p is 5790m/s , c_s is 3200m/s, steel plate thickness is 10mm and the preset frequency range is from 0MHz to 2MHz.

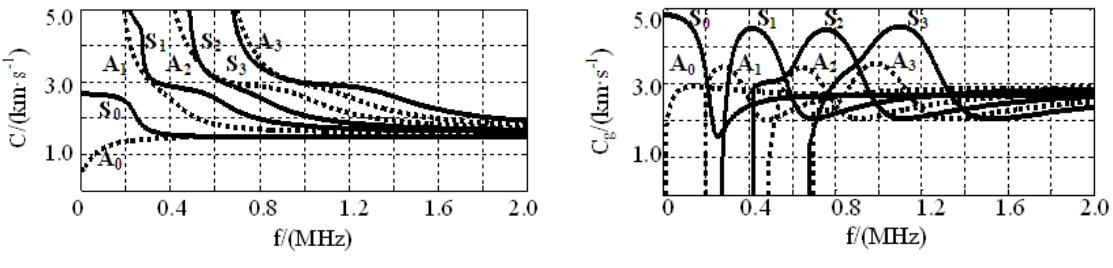

FIGURE 1. Four orders dispersion curves: (a) phase velocity, (b) group velocity

It is convenient from the dispersion curves to get the velocity of any mode under the frequency range concerned. It shows that the high order modes will appear only when the frequency is set at a certain value. Therefore, the two modes A_0 and S_0, frequency below 200kHz, have enough energy and weak dispersion. Hence, based on the measured wave modals, the localization algorithm can improve localization accuracy.

3. **NFM Localization Algorithm.** The definition of near field source can be expressed as $|r| \leq 2d^2/\lambda$, where $|r|$ is the distance form source to sensor, d is the aperture array of sensors and λ is the operating wavelength. The basic principle of near-field beamforming is described in Figure 2. Source 1 and source 2 are preset AE sources in twice test respectively. The output of these incident spherical waves can be illustrated by Equation (3), where m is the number of the sensors, and $x_n(t)$ is the records from the n-th sensor. w_n is the weighting coefficient for the channel of the n-th sensor, $\mathbf{w}(\mathbf{r}, \boldsymbol{\theta})$ is the direction and distance vector from sensors to AE source, and furthermore, $\mathbf{r_{k1}}$ and $\boldsymbol{\theta_{k1}}$ are the distance and the angle of arrival from the k-th AE source to the referenced sensor separately.

$$y(\mathbf{r}, t) = \frac{1}{m}\sum_{n=1}^{m} w_n x_n(t) = \frac{1}{m}\sum_{n=1}^{m} s_n(t)$$

$$\begin{aligned} &\mathbf{w}(\mathbf{r}, \boldsymbol{\theta}) \\ &= [w_1, w_2, \cdots, w_m] \\ &= \left[1 \quad e^{-j2\pi f_0 \frac{\sqrt{\mathbf{r}_{k1}^2 + d^2 - 2\mathbf{r}_{k1} d \sin\boldsymbol{\theta}_{k1}} - \mathbf{r}_{k1}}{c}} \quad \cdots \quad e^{-j2\pi f_0 \frac{\sqrt{\mathbf{r}_{k1}^2 + (m-1)d^2 - 2\mathbf{r}_{k1}(m-1) d \sin\boldsymbol{\theta}_{k1}} - \mathbf{r}_{k1}}{c}}\right]^T \end{aligned} \tag{3}$$

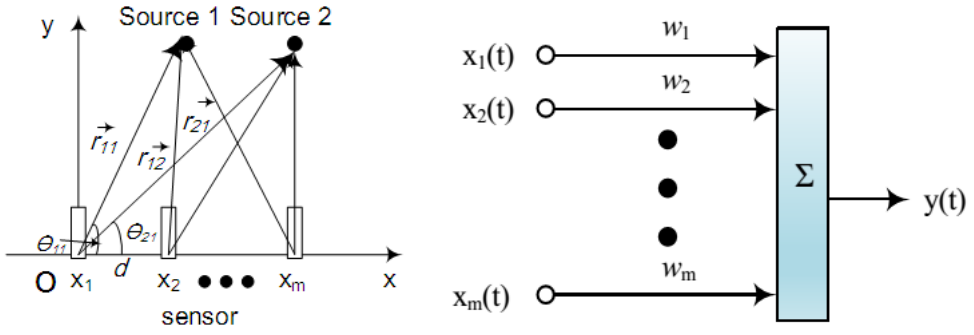

(a) (b)

FIGURE 2. Illustration of NFM model: (a) schematic diagram, (b) sensor array model

Multiple Signal Classification algorithm can decompose the acquired AE data into signal subspace and noise subspace, where the maximum eigenvector and eigenvalue correspond to the signal subspace and the others mean noise subspace. According to these subspace matrices, the angle and the distance of arrival can be estimated. The signal association matrix should be defined as

$$\mathrm{R_{ss}} = \frac{1}{N}\sum_{n=1}^{N} S(n) S^{\mathrm{H}}(n) \tag{4}$$

The covariance matrix can be eigenvalue decomposed as

$$\mathrm{R_{ss}} = \mathrm{U}\Sigma\mathrm{U}^{\mathrm{H}} = \mathrm{R_{xx}} + \mathrm{R_{nn}} = \mathrm{U_{xx}}\Sigma_{\mathrm{xx}}\mathrm{U_{xx}^{H}} + \mathrm{U_{nn}}\Sigma_{\mathrm{nn}}\mathrm{U_{nn}^{H}} \tag{5}$$

$\mathrm{R_{xx}}$ is the autocorrelation matrix due to signal without noise and $\mathrm{R_{nn}}$ is the autocorrelation matrix due to noise. Based on the condition, noise and signal are independent of

each other, the signal subspace orthogonal with noise subspace.

$$\mathbf{w^H}(\mathbf{r},\boldsymbol{\theta})\mathrm{U_n} = 0 \tag{6}$$

Then the multiple signal classification spectrum is presented below:

$$\mathrm{P}(\mathbf{r},\boldsymbol{\theta}) = \frac{1}{\mathbf{w^H}(\mathbf{r},\boldsymbol{\theta})\mathrm{R_{nn}}\mathbf{w}(\mathbf{r},\boldsymbol{\theta})} \tag{7}$$

As the denominator of $\mathrm{P}(\mathbf{r},\boldsymbol{\theta})$ approximates at zero, the spectrum approaches to the peak. Then the parameters $\boldsymbol{\theta}$ and $\mathbf{r}$ updated constantly, and the peak is the goal to locate the AE source.

$$\begin{aligned} \boldsymbol{\theta} &= \arg_{\boldsymbol{\theta}} \max \frac{1}{\mathbf{w^H}(\mathbf{r},\boldsymbol{\theta})\mathrm{R_{nn}}\mathbf{w}(\mathbf{r},\boldsymbol{\theta})} \\ \mathbf{r} &= \arg_{\mathbf{r}} \max \frac{1}{\mathbf{w^H}(\mathbf{r},\boldsymbol{\theta})\mathrm{R_{nn}}\mathbf{w}(\mathbf{r},\boldsymbol{\theta})} \end{aligned} \tag{8}$$

4. **Experiment Analysis.** In order to test the localization performance of the NFM method, the test table of the rotary machine rubbing experiment was carried out in Figure 3. As it is shown, four AE sensors were arranged in a line at the end of the case made by 10mm thick, arch steel plate. The coordinate origin was placed in the left of the linear sensor array and the aperture array was 50mm. In the test, the rubbing screw rubbed the rotor at preset position, and the AE acquisition system made by PAC Corporation, recorded test data at the sampling frequency 10MHz and with 60dB pre-amplifier to obtain optimal AE records.

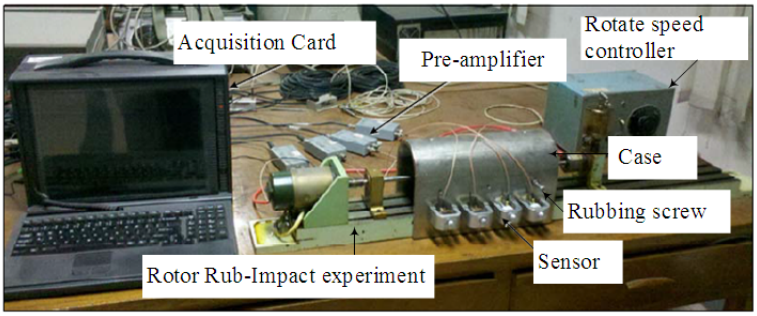

FIGURE 3. Experimental setup of the rotary machine

The AE energy in Figure 4(a) is gradually attenuated before the next rubbing occurs during the experiment. The amplified waveform of the signal in Figure 4(b) describes that the main energy of the previous AE signal has attenuated before next rubbing reaches. It is a stringent tendency to overlap the S and A waves together in each AE event.

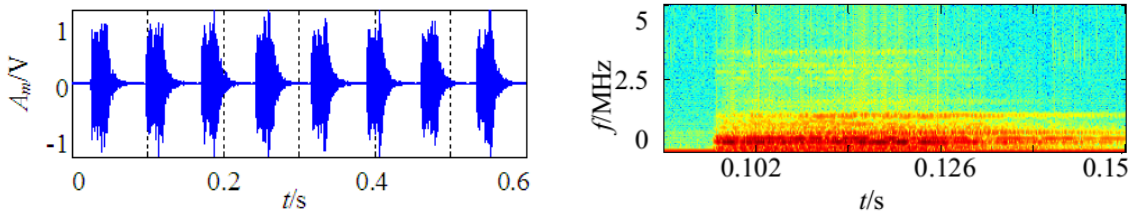

(a) (b)

FIGURE 4. Rubbing AE signal: (a) waveform in time domain, (b) magnified spectrogram

4.1. **WPT for S_0 and A_0 extraction.** To solve the overlap problem, based on the dispersion characteristics in Figure 1, the optimal WPT can be selected to extract A_0 and S_0 modes. Hemmati F demonstrated that the WPT for rubbing fault diagnostic utilizing Daubechies11 (Db11) orthogonal mother wavelet to decompose the signal into 9 levels presented an optimal SNR [12].

Figure 5(a) presents that each envelope peak is the arrival time of a wave travelling with the group velocity. As mentioned before, the first envelope peak is S_0 and the second envelope peak is A_0. Figure 5(b) describes the first large energy plots as the correspondence frequency f_0 in localization AE source. Considering the dispersion effect, based on the defined f_0, the revised velocity is defined as the group velocity of S_0 calculated from the dispersion curves in Figure 1 [9].

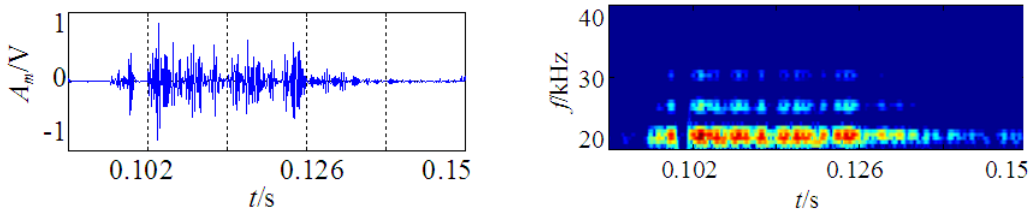

(a) (b)

FIGURE 5. Reconstructed each AE event: (a) waveform in time domain, (b) spectrogram

4.2. **NFM algorithm localization results.** Figure 6 shows the localization results based on the NFM, TOA, Delta-T and DTB methods. Three events at each preset source location are required to provide an average result and move erroneous data away.

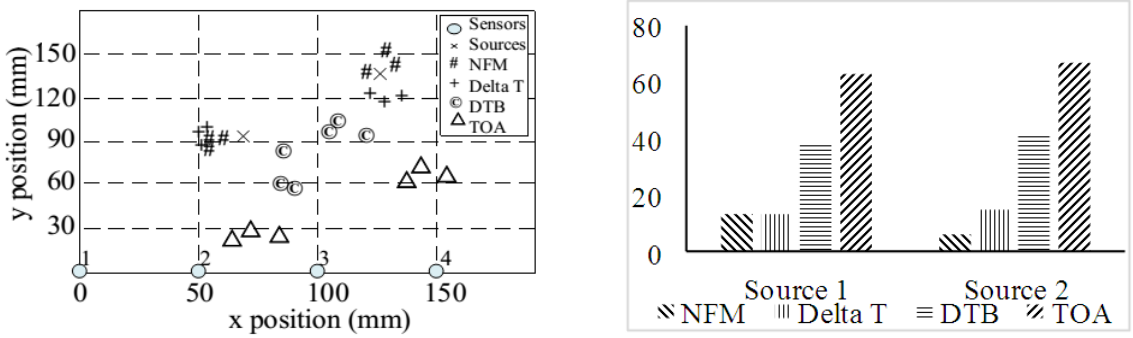

(a) (b)

FIGURE 6. Comparison with the NFM, TOA, Delta-T and DTB methods: (a) localization results (mm), (b) source localization RMS errors (mm)

It is clearly shown that the NFM and Delta-T obtain more accurate localization results than TOA and DTB methods. The reasons are that the revised wave velocities are close to the actual value and some noise effects are filtered away. Besides, the computational complexity of NFM is superior to Delta-T since NFM can be executed without grids and H-N source for training data for initial location mapping in Delta-T.

Figure 6(b) presents the average NFM localization RMS error compared with the other three methods. However, NFM localization approach provides the most precise results in the experimentation. Therefore, NFM method can be applied to monitor the sole rubbing fault source in rotary machine.

5. **Conclusion.** This paper proposes a novel NFM algorithm into detecting AE source in rotor rubbing. The superiorities of this algorithm to traditional methods are the extracted S_0 and A_0 through MPWT and WPT for overcoming dispersion effect and revised velocity, the following NFM algorithm for weakening the noise effects and increasing computational efficiency. The experiment results show that NFM can be considered as the best candidate for AE source localization methodology to be utilized for the fatigue location diagnosis of rotor rubbing in rotary machine. Further work aims to complete the workability of this method for detection multi-sources in rubbing and impacting.

Acknowledgements. This work is supported by the National Natural Science Foundation of China (no. 61201326, no. 61273266, no. 61375028). The authors thank all reviewers and editors, whose comments help improve the presentation of this work.

REFERENCES

[1] P. S. Keogh, Contact dynamic phenomena in rotating machines: Active/passive considerations, *Mechanical Systems and Signal Processing*, vol.29, no.5, pp.19-33, 2012.

[2] R. K. Miller and P. McIntire, *Acoustic Emission Testing*, NDT Handbook, American Society of Nondestructive Testing, 1987.

[3] P. Kundu, N. K. Kishore and A. K. Sinha, A non-iterative partial discharge source location method for transformers employing acoustic emission techniques, *Applied Acoustics*, vol.70, no.11, pp.1378-1383, 2009.

[4] M. Ahadi and M. S. Bakhtiar, Leak detection in water-filled plastic pipes through the application of tuned wavelet transforms to acoustic emission signals, *Applied Acoustics*, vol.71, no.7, pp.634-639, 2010.

[5] S. Mohd, *Acoustic Emission for Fatigue Crack Monitoring in Nuclear Piping System*, Ph.D. Thesis, Cardiff University, 2013.

[6] M. G. Baxter, R. Pullin and K. M. Holford, Delta T source location for acoustic emission, *Mechanical Systems and Signal Processing*, vol.21, no.3, pp.1512-1520, 2007.

[7] S. Mohd, K. M. Holford and R. Pullin, Acoustic emission source location in steel structures using a wavelet transform analysis and modal location theory, *Proc. of the 30th European Conference on Acoustic Emission Testing*, Spain, pp.1210-1221, 2012.

[8] G. C. McLaskey, S. D. Glaser and C. U. Grosse, Beamforming array techniques for acoustic emission monitoring of large concrete structures, *Journal of Sound and Vibration*, vol.329, no.12, pp.2384-2394, 2010.

[9] T. He, D. Xiao and Q. Pan, Analysis on accuracy improvement of rotor-stator rubbing localization based on acoustic emission beamforming method, *Ultrasonics*, vol.54, no.1, pp.318-329, 2014.

[10] J. L. Rose, *Ultrasonic Waves in Solid Media*, Cambridge University Press, London, 2004.

[11] B. Li, P. Duan and L. Qiang, A graphical edge method to solve dispersion equation of Lamb waves, *Proc. of the 1st Symposium on Aviation Maintenance and Management – Volume I*, 2014.

[12] J. L. F. Chacon, V. Kappatos, W. Balachandran et al., A novel approach for incipient defect detection in rolling bearings using acoustic emission technique, *Applied Acoustics*, vol.89, pp.88-100, 2015.